Materials Research. 2016; 19(6): 1299-1303
DOI: http://dx.doi.org/10.1590/1980-5373-MR-2016-0340

Syntheses and Fundamental Properties of Cr/Mo-Adoped Fe-Rich Alloys With Metastable Phase and Saturation Magnetization Near 1.9 T

Jian Ding[a], Ye Han[a], Fanli Kong[b], Akihisa Inoue[a,b,c], Shengli Zhu[a]*

[a] *School of Material Science and Engineering, Tianjin University, Tianjin, China*
[b] *International Institute of Green Materials, Josai International University, Togane, Japan*
[c] *Department of Physics, King Abdulaziz University, Jeddah 22254, Saudi Arabia*

Received: April 30, 2016; Revised: July 03, 2016; Accepted: August 26, 2016

The Fe-rich alloys of $Fe_{90-x}Si_5B_5M_x$ (M= Cr or Mo; x=1, 2) are synthesized in the present study. The as-spun structure mainly consists of bcc phase plus a minor amount of metastable phase (Fe_3B and/or $Fe_{23}B_6$). Comparing with the base alloy $Fe_{90}Si_5B_5$, the corrosion resistance is improved significantly due to the formation of the passive film. Saturation magnetic flux density reaches 1.9 T for the melt-spun alloys $Fe_{89}Mo_1Si_5B_5$. The alloys present a nearly constant high permeability in a rather high magnetic field up to coercive field which can be used as a new kind of sensor material with good fundamental properties and low cost.

Keywords: *Fe-rich metastable alloys; Magnetic sensor materials; High Bs; Corrosion resistance*

1. Introduction

Recently, there has been an increasing emphasis on the development of magnetic component with high performance and high integration level, which requires the exhibition of high saturation magnetic flux density (B_s) in combination with good mechanical strength and corrosion resistance for soft and hard magnetic materials[1]. In our previous study, we have been developing amorphous[2,3] and nanocrystalline[4] soft magnetic alloys and nanocomposite hard magnetic alloys[5] with B_s which is much higher than that of the commercialized composition in conjunction with good fundamental performance such as good corrosion resistance, wear resistance and bending ductility even after annealing.

Meanwhile, a series of Fe-rich crystalline-based $Fe_{90}Si_{10-x}B_x$ (x=2.5~7.5) alloys were developed as well[6]. These alloy ribbons consist mainly of bcc phase plus a minor mount of metastable phase such as amorphous and Fe_3B phase. Besides, the alloys exhibit unique magnetic properties of high B_s exceeding 1.9 T, moderately large coercivity (H_c) in conjunction with the nearly linear *B-H* relation in coercive field. In addition, these alloys show good bending ductile nature even after annealing. Such alloys are expected to provide unique magnetic behavior in moderately wide magnetic field for highly integrated magnetic sensor component.

However, their crystalline-based feature results in the low corrosion resistance than that of the Fe-Si-B amorphous alloy ribbons. This situation limits the application and increase in cost as a new kind of magnetic material. Therefore, there is a strong demand on improving the corrosion resistance for such alloys. It is expected to obtain the combination of such good properties by compositional modification. The study of Cr-adopted Fe-Si steel and Cr, Mo-adopted amorphous / glassy alloys indicate that the corrosion resistance can be improved by a small addition of Cr/Mo element[7-9]. On the contrary, however, the B_s value decreases simultaneously[10,11].

Based on our recent research of $Fe_{90}Si_5B_5$ alloy, Fe-rich alloys of 1 and 2 at% Cr / Mo substituted for Fe, i.e. $Fe_{90-x}Si_5B_5M_x$ (M=Cr or Mo; x=1, 2) are synthesized with the aim of improving the corrosion resistance and mechanical properties with no significant decrease in B_s in the present study.

2. Experiment procedure

Quaternary alloys $Fe_{89}Cr_1Si_5B_5$, $Fe_{88}Cr_2Si_5B_5$, $Fe_{89}Mo_1Si_5B_5$ and $Fe_{88}Mo_2Si_5B_5$ ribbons were prepared for this study. Their alloy ingots were prepared by arc melting the mixtures of pure elements in an argon atmosphere. Rapidly solidified ribbons were prepared by melt spinning and the resulting alloy ribbons have a thickness of about 20μm and a width of about 0.8 to 1.0 mm. The structure was examined by X-ray diffraction (XRD) with Cu-Kα radiation and transmission electron microscopy (TEM). XRD patterns were obtained on the free solidified side of the ribbon samples. Mechanical properties were measured by tensile testing machine (WDW-20) at room temperature. Tensile specimens had a gauge length of 10 mm in length and the strain rate was 0.05 s^{-1}. Bending ductility was evaluated by bending the specimen through 180 degrees. The bent surface was examined by scanning electron microscopy (SEM). The B_s and H_c were measured with a vibrating sample magnetometer (VSM) under a field of 800 kA/m and a DC B-H loop tracer under a field of 800 A/m, respectively. Corrosion behavior was evaluated for the ribbon samples which were degreased, washed and dried in air

* e-mail: hanye0704@yahoo.com

before immersion by electrochemistry test. Electrochemistry measurements were performed by an electrochemistry workshop (Gamry Reference 600 redefining electrochemical measurement) in 3.5mass% NaCl solution at 298 K. Ribbon samples were set as working electrode; a platinum electrode was working as counter electrode and a saturated calomel electrode (SCE) was used as reference electrode. Polarization curves were measured by a potentiodynamic process from 250mV under open circuit potential (OCP) to 250mV above OCP value at a scanning rate of 1mV/s.

3. Results and Discussion

Figure 1 (a) shows the X-ray diffraction patterns of the present melt-spun ribbons. The major phase in these alloys is identified as bcc-Fe from the ordinary XRD patterns. Besides, one can notice tiny peaks around 44 degree in the diffraction patterns of all alloys, which can be indexed as Fe_3B phase[6]. This resulted structure is similar to that of the $Fe_{90}Si_5B_5$ alloy. Besides, from the high resolution XRD pattern of $Fe_{88}Mo_2Si_5B_5$ alloy shown in Figure 1 (b), it can be recognized the tiny peak appeared around the (110) peak of bcc-Fe, indicating the presence of another phase, which will be discussed later.

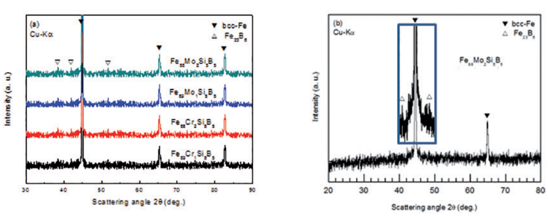

Figure 1: (a) X-ray diffraction pattern of $Fe_{90-x}Si_5B_5M_x$ (M=Cr, Mo; x=1, 2) alloys with Cu-Kα radiation. (b) high resolution scanned XRD patterns of $Fe_{88}Mo_2Si_5B_5$ alloy.

In order to clarify the structure feature and phase component in details, the $Fe_{88}Mo_2Si_5B_5$ alloy was studied by TEM. Figure 2 shows the bright-field TEM images and SAED patterns of $Fe_{88}Mo_2Si_5B_5$ alloys. The as-spun structure consists of bcc phase with a grain size of about 0.1 to 0.2 μm and nearly fine spherical precipitates with a size of about 20 nm. The diffraction patterns shown in Figure 2 (b) and (c) are identified as bcc-Fe and fcc-$Fe_{23}B_6$ phases, respectively. $Fe_{23}B_6$ is a metastable boride phase present in different kind of steel and alloys. It can easily decompose into bcc-Fe and Fe-B. However, this phase is stabilized when Fe atom site is partially substituted by another transition metal atom[12]. The larger atomic radius of Mo (0.140 nm) and the strong Mo-B interaction is deduced to impede the atomic migration for the decomposition of $Fe_{23}B_6$ phase. Thus the as-spun structure is composed of bcc + Fe_3B phase for $Fe_{89}Cr_1Si_5B_5$, $Fe_{88}Cr_2Si_5B_5$, and $Fe_{89}Mo_1Si_5B_5$ alloys as well as bcc + Fe_3B phase + $Fe_{23}B_6$ phase for $Fe_{88}Mo_2Si_5B_5$ alloy, respectively.

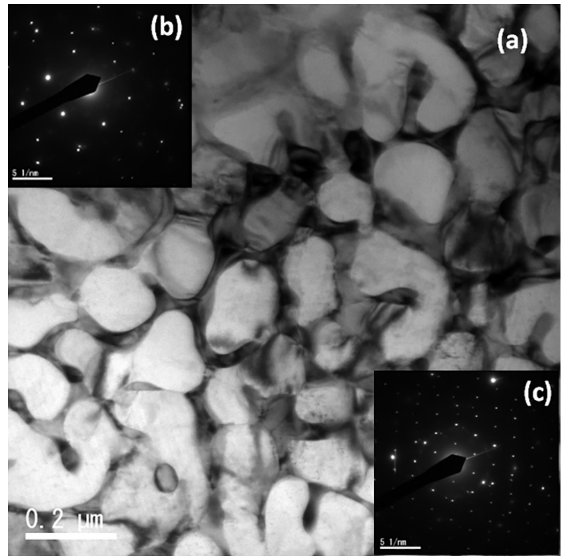

Figure 2: (a) Bright-field and (b) (c) selected area electron diffraction patterns in different phases of the $Fe_{88}Mo_2Si_5B_5$ alloy.

All the present as-spun alloy ribbons are ductile, which means the ribbons can not be bent into two pieces, and their ductility maintains even after annealing. Figure 3 (a) shows the surface appearance of the $Fe_{89}Mo_1Si_5B_5$ alloy ribbon annealed at 823 K for 600 s subjected to the bending deformation through 180 degrees. The ribbon does not crack into two pieces. In order to examine the deformation behavior in details, the crease marks were observed with a SEM (Figure 3(b)). The surface shows a number of shear bands, revealing its excellent bending ductility. It is well known that for some soft magnetic nanocrstalline alloys such as FINEMET, the volume fraction of the nanocrystalline phase is very large, reaching a value of almost 90%[13]. However, their exhibiting of nearly unavoidable bending brittleness limits the utilizing of such soft magnetic alloys in engineering fields. For the present Fe-rich quaternary alloys, however, good bending ductility can be obtained though the major phase is also crystalline.

Figure 4 shows the *B-H* hysteresis loops for the present Fe-Si-B-TM alloys in as-spun state, and the B_s and H_c of the alloys annealed at 823 K for 600 s are summarized in Table 1. For the as-spun ribbons, the $Fe_{89}Mo_1Si_5B_5$ ribbon exhibits the highest B_s value, and then followed by $Fe_{89}Cr_1Si_5B_5$. Adding 2 at% Mo does not affect as harmful as 2 at% Cr on the B_s value, which is presumably due to the presence of the remaining $Fe_{23}B_6$ phase. According to recent theoretical studies about the structure and magnetic properties of $Fe_{23}M_6$-type phase (M=C or B) using first-principles theory[14], it is revealed that the $Fe_{23}M_6$ phase has strong ferromagnetic characteristics and large magnetic moment. After annealing, the $Fe_{89}Mo_1Si_5B_5$ alloy maintains high B_s value of 1.9 T in spite of the presence of Fe_2B precipitates. Besides, these Fe-rich crystal-based alloys exhibit moderately large coercivity,

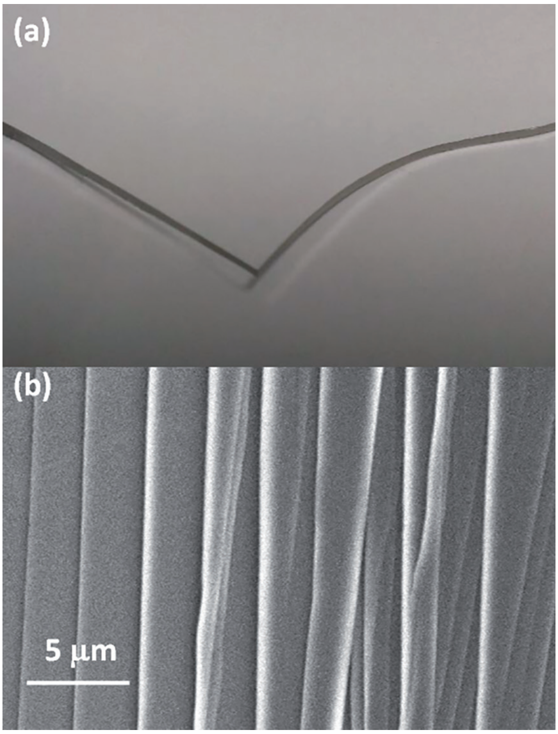

Figure 3: (a) outer surface and (b) SEM image obtained near the crease mark of the bent alloy ribbon $Fe_{88}Mo_2Si_5B_5$ annealed at 823 K for 600 s.

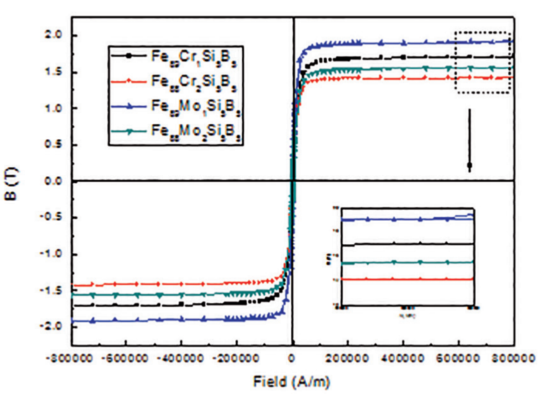

Figure 4: *B-H* hysteresis loops of $Fe_{90-x}Si_5B_5M_x$ (M=Cr, Mo; x=1, 2) ribbon as-spun alloys under an applied field of 800 kA/m.

which is related to the irregular shape and wide size range of the grains to obtain significant magnetic anisotropy. As recognized previously, the present alloys maintain the unique magnetic features of showing a nearly constant permeability (slope) up to relatively high magnetic field corresponding to a moderately large coercivity.

Figure 5 shows the polarization curves of the annealed ribbons and their electrochemistry parameters are summarized in Table 1. By addition of Cr or Mo into the $Fe_{90}Si_5B_5$ alloy (I_{corr}=15.65 A/cm^2, E_{corr}=-0.796 V), the corrosion current density decreased by and order of magnitude and the corrosion potential distinct increased as well. Moreover, one can notice that among these alloys, composition containing Cr exhibit relatively lower corrosion current and higher corrosion potential than those of the Mo-containing alloys, which is caused by the formation of stable protective passive films made of Cr-rich oxides[8]. Although Cr and Mo belongs to the same subgroup in the periodic table which seems to exhibit the similar chemical properties, stable Mo-rich passive film cannot form on the surface deducing by the low Mo content than normal level detected by XPS[15]. This can be explained by the difficulty of atomic migration of Mo to the surface resulting from the stronger bond than Cr to other metalloid elements due to the larger atomic radius. It is thus can be concluded that by adopting 1 at% to 2 at% of Cr and Mo, the corrosion resistance is improved significantly as compared with the base alloy $Fe_{90}Si_5B_5$.

The mechanical strength of the present alloy ribbons are estimated by tensile test. The obtained mechanical properties parameters such as tensile fracture strength, elongation of the annealed alloys are summarized in Table 1. Comparing with the base alloy $Fe_{90}Si_5B_5$ (1028 MPa), the tensile fracture strength has been significantly increased. The reason for the annealing-induced enhancement of mechanical strength can be regarded caused by the changes of structure feature. Figure 6 (a) shows the high resolution XRD patterns of the annealed $Fe_{88}Mo_2Si_5B_5$ alloy. Tiny peaks besides the bcc-Fe (110) peak can be recognized, which are indexed as precipitated Fe_2B and remaining Fe_3B phase. Figure 6 (b) shows the TEM bright-field image of this annealed alloy. One can notice the growth of the compound phase from

Table 1: Saturation magnetic flux density (B_s), coercivity (H_c), corrosion current density (I_{corr}), corrosion potential (E_{corr}), tensile fracture strength (σ_f) and elongation rate (ε) of the $Fe_{90-x}Si_5B_5M_x$ (M= Cr or Mo; x=1, 2) alloys annealed at 823 K for 600 s.

Alloy Composition	B_s (T)	H_c (A/m)	I_{corr} (µA/cm^2)	E_{corr} (V)	σ_f (MPa)	ε (%)
$Fe_{89}Cr_1Si_5B_5$	1.68	189	7.1	-0.716	1151	0.363
$Fe_{88}Cr_2Si_5B_5$	1.49	654	6.7	-0.683	1158	0.444
$Fe_{89}Mo_1Si_5B_5$	1.90	790	9.7	-0.738	1250	0.373
$Fe_{88}Mo_2Si_5B_5$	1.63	945	9.4	-0.799	1380	0.575

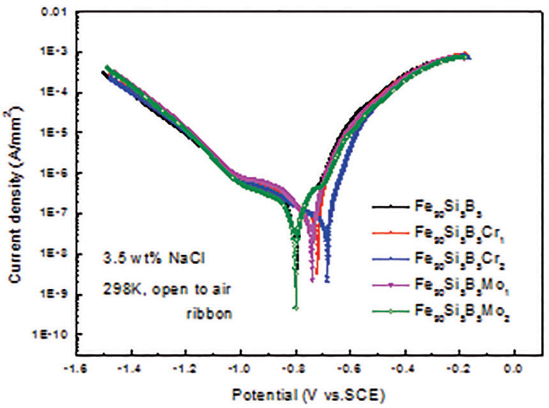

Figure 5: Polarization curves of the $Fe_{90-x}Si_5B_5M_x$ (M= Cr or Mo; x=1, 2) ribbon alloys in 3.5mass% NaCl solution at 298K. The ribbons were annealed at 823 K for 600s.

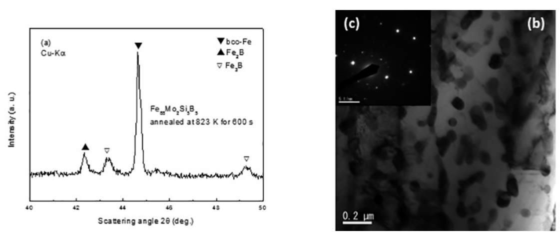

Figure 6: (a) High resolution XRD patterns (Cu-Kα) and (b) Bright-field image with corresponding (c) selected area electron diffraction pattern of $Fe_{88}Mo_2Si_5B_5$ ribbon after annealing at 823 K for 600 s.

20 nm (as-spun state) to 80 nm (annealed state). Thus the enhancement of mechanical strength is caused by the growth of Fe-B compound. Besides, here it is necessary to point out that the suitable growth of Fe-B precipitate is not harmful for the alloys to exhibit good bending ductility.

4. Conclusion

We examined the formation, structure, mechanical properties, magnetic properties as well as corrosion resistance of the alloys with the composition of $Fe_{90-x}Si_5B_5M_x$ (M=Cr or Mo; x=1, 2). The results obtained are summarized as followed:

1. The as-spun structure is composed of bcc + Fe_3B phase for $Fe_{89}Cr_1Si_5B_5$, $Fe_{88}Cr_2Si_5B_5$, and $Fe_{89}Mo_1Si_5B_5$ alloys as well as bcc + Fe_3B + $Fe_{23}B_6$ phase for $Fe_{88}Mo_2Si_5B_5$ alloy, respectively.
2. All as-spun ribbon samples exhibit good bending ductility in as-spun state and even after annealing. Tensile fracture strength of the present alloys increased after annealing, caused by the growth of the Fe-B compound phase.
3. Corrosion resistance has been improved significantly by adopting Cr to the base alloy $Fe_{90}Si_5B_5$, contributing from the formation of the stable Cr-rich passive film.
4. High B_s of 1.9 T is obtained for the present study, in conjunction with moderately large coercivity. Besides, all samples present a nearly constant high permeability in a rather high magnetic field up to coercive field which can be useful for special application in a rather wide magnetic field.

5. Acknowledgements

The present research is supported by China Postdoctoral Science Foundation (2014M560186), JSPS KAKENHI Grant in Japan (26630299) and Recruitment Program of Global Experts “1000 Talents Plan” of China (WQ20121200052).

6. References

1. Inoue A, Kong FL, Man QK, Shen BL, Li RW, Al-Marzouki F. Development and applications of Fe- and Co-based bulk glassy alloys and their prospects. *Journal of Alloys and Compounds*. 2014;615(Suppl 1):S2-S8.

2. Kong FL, Chang CT, Inoue A, Shalaan E, Al-Marzouki F. Fe-based amorphous soft magnetic alloys with high saturation magnetization and good bending ductility. *Journal of Alloys and Compounds*. 2014;615:163-166.

3. Han Y, Kong FL, Chang CT, Zhu SL, Inoue A, Shalaan ES, et al. Syntheses and corrosion behaviors of Fe-based amorphous soft magnetic alloys with high-saturation magnetization near 1.7 T. *Journal of Materials Research*. 2015;30(4):547-555.

4. Makino A, Men H, Kubota T, Yubuta K, Inoue A. New Fe-metalloids based nanocrystalline alloys with high B_sBsof $1.9T$ and excellent magnetic softness. *Journal of Applied Physics*. 2009;105:07A308.

5. Zhou W, Chang C, Inoue A, Wang X, Li F, Huo J. Direct production of hard magnetic ribbons with enhanced magnetic properties by controlling cooling rate of melt. *Journal of Applied Physics*. 2015;117:123905.

6. Han Y, Kong F, Chang C, Zhu S, Ketov S, Louzguine D, Inoue A. Syntheses and Fundamental Properties of Fe-rich Metastable Phase Alloys with Saturation Magnetization Exceeding 1.9 T. Materials Research. 2015:18 Suppl. 1:127-135.

7. Takagi S, Matsuzaki A, Yamashita T, Sumiyama K. Japanese Patent, Kawasaki Steel Co. (1997), JPH1150204A.

8. Pang S, Zhang T, Asami K, Inoue A. Effects of Chromium on the Glass Formation and Corrosion Behavior of Bulk Glassy Fe-Cr-Mo-C-B Alloys. *Materials Transactions*. 2002;43(8):2137-2142.

9. Shen B, Akiba M, Inoue A. Effect of Cr addition on the glass-forming ability, magnetic properties, and corrosion resistance in FeMoGaPCBSi bulk glassy alloys. *Journal of Applied Physics*. 2006;100(4):043523.

10. Chen W, Liu J, Cheng Z, Lin X, Zhu J. Effect of Chromium on Microstructure, Ordered Phase and Magnetic Properties of Fe-6.5 wt%Si Alloy Effect of Chromium on Microstructure, Ordered Phase and Magnetic Properties of Fe-6.5 wt%Si Alloy. *Materials Today: Proceedings*. 2015;2(Suppl 2)Supplement 2,:S314-S318.

11. Pawlik P, Davies HA. The bulk glass forming abilities and mechanical and magnetic properties of Fe–Co–Zr–Mo–W–B alloys. *Journal of Non-Crystalline Solids*. 2003;329(1-3):17-21.

12. Imafuku M, Sato S, Koshiba H, Matsubara E, Inoue A. Structural variation of Fe-Nb-B metallic glasses during crystallization process. *Scripta Materialia*. 2001;44(8-9):2369-2372.

13. Suryanarayana C, Inoue A. *Bulk metallic glasses*. New York: CRC Press; 2011.

14. Fang CM, van Huis AM, Sluiter MHF, Zandbergen HW. Stability, structure and electronic properties of γ-$Fe_{23}C_6$ from first-principles theory. *Acta Materialia*. 2010;58(4):2968-2977.

15. Pang SJ, Zhang T, Asami K, Inoue A. Bulk glassy Fe–Cr–Mo–C–B alloys with high corrosion resistance. *Corrosion Science*. 2002;44(8):1847-1856.